ACS OMEGA

Open Access

http://pubs.acs.org/journal/acsodf

Article

Numerical Study of the Combustion Characteristics of an 800−1200 kW High-Power Porous Media Combustor at Atmospheric Pressure

Riyi Lin,* Wei Li, Huanan Li, Xinxin Liu, Jitao He, and Xinwei Wang

Cite This: *ACS Omega* 2024, 9, 31384−31392

Read Online

ACCESS | Metrics & More | Article Recommendations

ABSTRACT: Porous media combustion has the advantages of high combustion efficiency and low pollutant emissions. However, there are few studies on the combustion characteristics and pollutant emissions of high-power porous media combustion chambers and fire tubes. Based on the computational fluid dynamics method, the stable combustion characteristics and pollutant emission rules of methane-air were explored in a high-power porous media combustion chamber of 800−1200 kW. The results show that the combustion of the porous media combustor is stabilized at an inlet velocity of 0.8−1.6 m/s with an equivalence ratio of Φ = 0.5−0.9. The high-power porous medium combustor has the highest limiting temperature at Φ = 0.7. Temperature increases gradually with increasing porosity within the −2.5 to 1 m axial center interval. The outlet radial temperature distribution tends to be uniform with the increase of porosity, and the outlet temperature is highest for porous media with a thickness of 400 mm. NO emission was lowest at an inlet velocity of 1.2 m/s. A significant reduction in NO emissions was observed with increasing equivalence ratio. NO generation increases with increasing porosity at porosities between 0.75 and 0.85. NO generation increases with the thickness of the porous media and increases sharply at 600 mm. The results above can provide guidelines for the design of a high-efficiency high-power porous combustor.

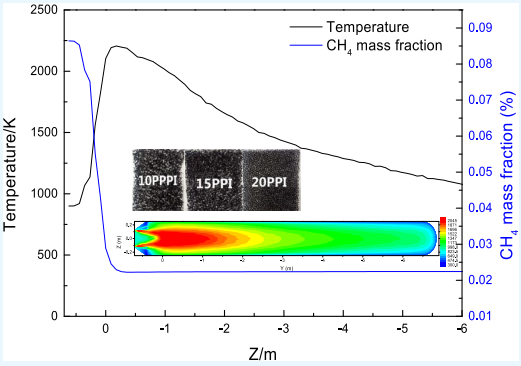

1. INTRODUCTION

With the rapid development of social economy, the energy consumption of various industries is increasing, and the accompanying environmental problems have become the focus of people's attention.[1] Porous media combustion (PMC) technology refers to the combustion process that occurs in the pores of inert porous media materials, which is one of the hot spots that scholars at home and abroad focus on.[2] In the combustion process within porous media, the heat released from the combustion of premixed gases is transferred to fresh premixed gases through the heat storage capacity of the porous media material, along with strong heat conduction and radiation effects.[3] This results in the highest flame temperature surpassing the adiabatic combustion temperature of the fuel in the traditional free space combustion. Consequently, porous media combustion exhibits the characteristic of "excess enthalpy".[4] Compared to traditional free space combustion, it offers advantages such as high combustion efficiency, a wide range of stable combustion, and reduced pollutant emissions, demonstrating significant potential for various applications.[5]

Porous media have good heat storage properties. Scholars have extensively studied the effect of small- and medium-sized porous media combustors on temperature distribution and flame characteristics. Zhdanok et al.[6] studied the effect of equivalence ratio on the change of packed bed temperature with time and found that the maximum temperature was 2.8 times the normal adiabatic temperature. Bakry et al.[7] investigated the combustion characteristics of premixed gases in a new porous media combustor (PMC). It was found that as the equivalence ratio increases, the propagation speed of the combustion wave decreases but the high-temperature zone increases. However, the operating parameters also influence the flame combustion characteristics. Hashemi et al.[8] studied the flame stability of methane-air premixed gas in a double-layer porous media combustor based on a two-dimensional model. It was found that not only did the maximum flame temperature increase with the increase of the equivalence ratio but also the flame steady combustion limit gradually increased. Zheng et al.[9] simulated the flame characteristics of methane and air in a combustor filled with alumina particles and analyzed the effect of different inlet velocities on the flame shape. It was found that the flame profile was relatively flat at lower inlet velocities, and the flame profile was parabolic as the inlet velocity increased. Shinoda[10] simulated the stable

Received: December 28, 2023
Revised: April 14, 2024
Accepted: July 1, 2024
Published: July 10, 2024

https://doi.org/10.1021/acsomega.3c10444
ACS Omega 2024, 9, 31384−31392

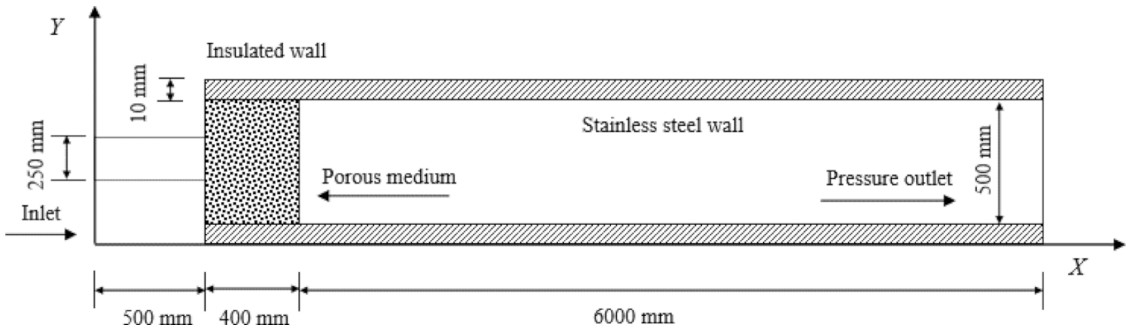

Figure 1. Schematic diagram of the porous combustor.

combustion range of methane premixed gas submerged combustion under different equivalence ratio conditions and found that the combustion stability deteriorates as the equivalence ratio is low. Yang et al.[11] carried out an experimental study on the premixed combustion process in a porous media consisting of ceramic particles and derived the law that the flame propagation velocity decreases with increasing equivalence ratio. Similarly, the structure of the porous media also has an effect on the temperature distribution. Yan et al.[12] investigated the effect of porous media porosity on the combustion temperature law. It was found that the temperature gradient between gas and solid becomes smaller with an increase in the pore density. Sasmal et al.[13] investigated the effect of pore size on the temperature distribution within the combustor in a flame-resident combustor. The results showed that when the pore size of the porous medium becomes smaller, the system reaches thermal equilibrium between the gas and the solid more quickly. When the pore size becomes larger, it leads to a lower maximum temperature of the gas. However, the structure of the porous medium also affects the flame combustion characteristics. Tang[14] investigated the effect of pore structure on combustion characteristics and found that when the pore density of the pore structure of the porous media is arranged in a stepwise manner, it can promote the combustion of the fuel in the combustion chamber. Chu et al.[15] investigated the laws affecting the pore size structure of porous media on combustion characteristics. It was shown that due to the change in pore size, the airflow disturbance in porous media increases, heat transfer between gas and solid is enhanced, flame stability is enhanced, and the range of stable combustion increases. Xie[16] explored the effect of porosity on combustion stability by numerical simulation. The results showed that the larger the porosity of the porous media, the more prone to blowout in the combustor. Wang et al.[17] studied the methane-air premixed combustion process and found that increasing the outlet diameter of the burner and the length of the preheating zone of the burner can significantly improve the stability limit of the burner. When the ratio of the length of the preheating zone to the length of the reaction zone is 0.33, the combustion conditions are most favorable.

Scholars have extensively studied the characteristics of pollutant emissions from small- and medium-sized porous media combustors. Gao et al.[18] investigated the relationship between pore density and pollutant emissions for porous media with a diameter of 50 mm and a length of 100 mm burner. The results showed that 30 PPI porous media produced higher pollutant CO due to lower combustion flame temperature compared to porous media with pore density less than 30 PPI. However, Shakiba et al.[19] found experimentally that as the porosity of porous media decreases, not only does the pollutant emission content increase but also the combustion efficiency decreases. After that, Kang et al.[20] studied the relationship between the pore arrangement structure of porous media and pollutant emissions and found that as the radial density decreases outward, the emission of CO in pollutants gradually increases. Similarly, changing the operating parameters will also have an impact on pollutant emissions. Khanna et al.[21] studied methane-air combustion in a porous media combustor with a diameter of 51 mm and a length of 90 mm. They conducted an experimental study and found that the NOx emissions remained constant over the range of inlet velocities studied. Dehaj et al.[22] investigated the testing of natural gas in a porous media combustor and found that NOx emissions from the combustion chamber were higher at small equivalence ratios. Mustafa et al.[23] conducted experiments on pollutant emissions from a porous media combustor at different equivalence ratios. As the equivalence ratio increased, the NOx emissions were less than 36 ppm, but the CO emissions were not satisfactory. It is difficult to minimize CO and NO emissions at the same time. Keramiotis et al.[24] studied the relationship between excess air coefficient and combustion characteristics and pollutant emissions and found that when the excess air coefficient was relatively small but the combustion temperature was high, the NOx content of pollutant emissions increased as the combustion intensity increased but as the excess air coefficient continued to increase, the pollutant emission content remained essentially unchanged. However, Fierro et al.[25] experimentally investigated the effect of equivalence ratios on pollutant emissions from a porous media combustor during methane-air combustion and found that pollutant emissions were low when equivalence ratios were low but gradually increased as equivalence ratios increased. Janvekar et al.[26] studied the combustion and preheating zones of a small burner with a diameter of 23 mm and a length of 100 mm. It was found that the optimum equivalence ratio of the surface flame was 0.7 and submerged combustion occurred at equivalence ratios lower than 0.6, the maximum temperature recorded at the optimum equivalence ratio was 620 °C, the maximum thermal efficiency was 81%, and the emission parameters such as nitrogen oxides and carbon monoxide were less than 1 ppm.

Although porous media combustion has good application prospects due to its advantages of full combustion, uniform temperature, stable flame, and low pollutant emission, the current porous media combustors are mostly focused on the laboratory level, with a power of less than 1000 kW. There is no in-depth study of the structural and operating parameters of

https://doi.org/10.1021/acsomega.3c10444
ACS Omega 2024, 9, 31384−31392

high-power porous media combustors. Therefore, this paper investigates the effects of equivalence ratio, inlet velocity, porosity, and thickness of porous media on the temperature distribution characteristics of methane combustion in porous media combustor, NO pollutant generation, and emission patterns under high-power conditions. The aim is to study the key parameters affecting the pollutant emission and temperature uniformity of high-power porous media combustors and to provide theoretical guidance for the design of high-power porous media combustors.

2. NUMERICAL MODEL

2.1. Physical Model. A methane-air premixed combustion porous media combustor was designed and modeled to burn methane fuel, as shown in Figure 1. The entire combustion chamber has a length of 6400 mm and a diameter of 500 mm, and the interior is filled with the inert material silicon carbide (SiC). To prevent the flame from overflowing from the porous media area, 10-mm-thick stainless steel is used as the shell.

2.2. Mathematical Model. To simplify the calculation, some assumptions are made as follows: (1) steady-state combustion, no gas radiation; (2) incompressible flows; (3) inert isotropic and homogeneous porous media; and (4) the heat transfer efficiency between the porous media and the gas is high, and the temperatures of the porous media and the internal flow gas are equal.[27] Based on the above assumptions, the conservation equations are written as follows:

Continuity equation:

$$\nabla(\varepsilon\rho_g\vec{u}) = 0 \tag{1}$$

The momentum equation:

$$\nabla(\varepsilon\rho_g u\cdot\vec{u}) = -\varepsilon\frac{\partial p}{\partial x} + \nabla(\mu\nabla u) + \frac{\mu}{C_1}u + \frac{\rho_g}{C_2}u^2 \tag{2}$$

$$\nabla(\varepsilon\rho_g V\cdot\vec{V}) = -\varepsilon\frac{\partial p}{\partial x} + \nabla(\mu\nabla V) + \frac{\mu}{C_1}V + \frac{\rho_g}{C_2}V^2 \tag{3}$$

Energy equation:

$$\nabla(\varepsilon\rho_g\vec{u}h) = \nabla(\lambda_{eff}\nabla T) - \sum_i h_i\omega_i W_i \tag{4}$$

where λ_{eff} is the effective thermal conductivity of porous media, $\lambda_{eff=}\ \varepsilon\lambda_g + (1-\varepsilon\lambda_s)$, and λ_g and λ_s are the thermal conductivities of porous media and gas, respectively.

Component transport equation:

$$\nabla(\varepsilon\rho_g\vec{u}Y_i) = \nabla[\varepsilon D_{im}\nabla(\rho Y_i)] + \varepsilon\omega_i W_i \tag{5}$$

2.3. Boundary Condition and Solving Method. The inlet of the model is set to the uniform velocity inlet. The external environment is set as 300 K. The initial temperature of the premixed gas is set as 850 K. The outlet pressure is set as 0. As shown in Figure 1, the inlet pipe wall is adiabatic, and the fire tube wall is nonadiabatic. The heat loss on the outer combustor wall is as follows:

$$q_w = h_n(T_W - T_\infty) + \varepsilon_W\sigma(T_W^4 - T_\infty^4) \tag{6}$$

where h_n is the heat transfer coefficient of stainless steel wall, 20 W/(m^2·K); T_∞ is the ambient temperature set to 300 K; the emissivity ε_w of T_w stainless steel wall is generally 0.9;[28] and the Stefan−Boltzmann constant is 5.67 × 10^{-8} W/(m^2·K^4).

Based on Mohamed's[29,30] simplified treatment of porous media foam ceramic structure and the mathematical model established on this basis, the expressions of viscous resistance coefficient C_1 and inertial resistance coefficient C_2 are obtained, respectively:

$$C_1 = \frac{32}{\varepsilon d_p^2} \tag{7}$$

$$C_2 = \frac{2F}{\sqrt{1/C_1}} \tag{8}$$

where d_p is the diameter of the skeleton of the cubic frame and C is the resistance coefficient of the porous media skeleton.

The thermal conductivity was selected as a function of temperature as provided in the literature[15] for the effective thermal conductivity of silicon carbide:

$$k_s = 0.34691\text{-}736.72 \times 10^{-6}T + 1.2052 \times 10^{-6}T^2 \tag{9}$$

The simulation results of methane combustion for the five-step mechanism and the detailed mechanism have good prediction accuracy for the flame temperature distribution.[33] In this study, we consider mainly the thermal type of NO generation. In order to calculate the efficiency and cost, the five-step mechanism is employed.[34,35] The turbulence model is solved by the standard k-turbulence finite rate model. The pressure−velocity coupling was solved by employing the SIMPLE algorithm. The second-order upwind scheme was used to discretize all of the equations. The convergence standard of the residual error of the energy equation is set as 10^{-6}. The convergence standard of the remaining equations is set as 10^{-3}. The thermal properties and diffusion parameters of the material are set based on Table 1.

Table 1. Physical Parameters of Porous Media[31,32]

pore density/PPI	pore diameter/mm	porosity	emissivity
20	1.0	0.75	0.9
15	1.5	0.80	0.9
10	1.8	0.85	0.9

2.4. Grid Independence Validation and Model Validation. To verify the reliability and validity of the porous media, a combustion model was used. Grid independence test and reliability verification were checked under three mesh densities as seen in Figure 2b. The simulations were carried out for three mesh sizes at an equivalence ratio of 1, an inlet velocity of 0.8 m/s, a porosity of 0.85, and a pore density of 10 PPI, and boundary conditions were set up according to Section 2.3. The central axial temperature distribution curves calculated by different grid sizes are compared, as shown in Figure 2b. As can be seen in Figure 2b, the temperature distribution curve for the mesh with 106620 cells has a larger error near the peak than the temperature curves for the other two mesh densities. The temperature distribution curve with the mesh with 210230 cells can better characterize the axial temperature distribution of the porous media combustor. The result of increasing the mesh with 361060 cells is very close to the calculation result of the mesh with 210230 cells. To save computational cost and meet the accuracy requirements, the mesh with 210230 cells was employed in the following simulations.

https://doi.org/10.1021/acsomega.3c10444
ACS Omega 2024, 9, 31384−31392

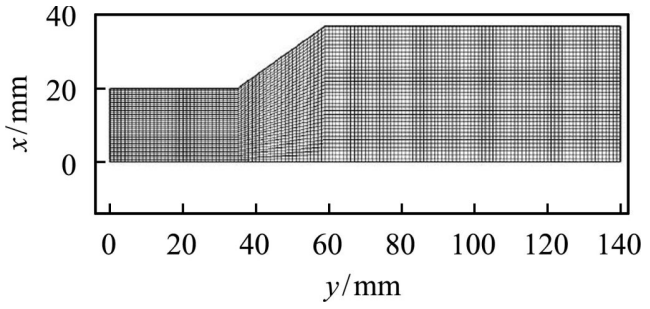

(a) Porous media combustor in the literature [8]

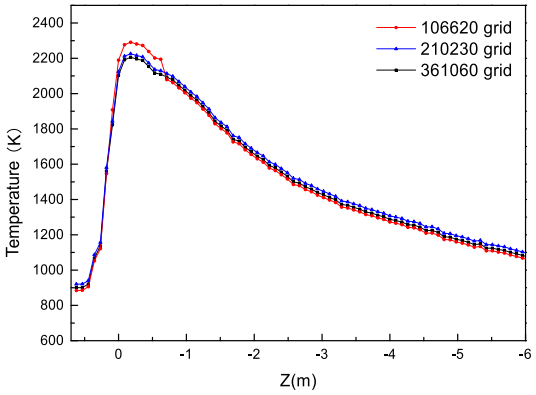

(b) Center axial temperature profiles of different mesh sizes

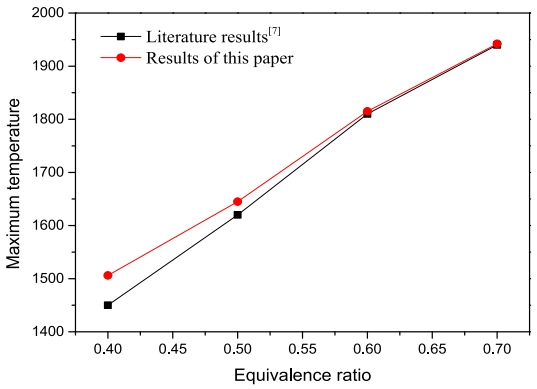

(c) Model validation

Figure 2. Grid independence validation and model validation.

To verify the reliability of the model used in this study, the same numerical model is developed according to the literature[8] and simulations are carried out according to the same initial and boundary conditions as in the literature. From Figure 2c, it can be seen that the maximum temperature of the stable combustion flame is essentially linear with the excess air coefficient compared to the literature results. The maximum error does not exceed 3.5% compared to the simulation results in the literature.[8] The reliability of the model was verified by the above comparison.

3. RESULTS AND DISCUSSION

3.1. Comparison of Thermal Performance. The temperature distribution characteristics of the combustor are key factors in measuring the combustion efficiency of the combustor. Therefore, the effect of different inlet velocities on the temperature distribution characteristics of the combustor under methane-air premixing conditions will be investigated in this section. Figure 3 shows the axial temperature and methane

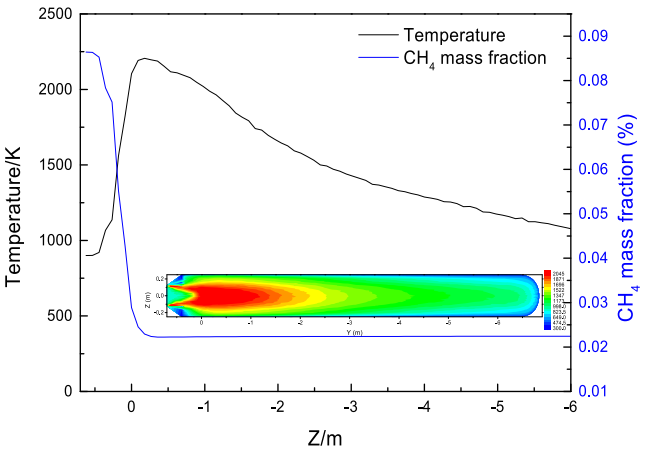

Figure 3. Center axial temperature and CH_4 mass fraction profiles of the combustor.

distribution in the high-power porous media combustor with a porosity of 0.85, a pore density of 10 PPI, an equivalence ratio of 0.5, and an inlet velocity of 0.8 m/s. From Figure 3, it can be seen that the axial temperature in the porous media section (Z = −0.4 to 0 m) reaches the limit value. A large amount of methane is burned, and a stable flame is formed in the fire tube.

3.1.1. Effect of Inlet Velocity and Equivalence Ratio. Figure 4 shows the temperature distribution in the fire tube at different inlet velocities. It can be seen from the figure that as the inlet velocity increases, the high-temperature area in the fire tube increases. The maximum temperature inside the flame increases from 1860 to 2026 K when the inlet velocity increases from 0.8 to 1.6 m/s. This is due to the increase in the inlet velocity, the increase in the amount of methane burned per unit of time, and the increase in heat output. Therefore, the temperature inside the fire tube increases. As the inlet velocity increases, the flame length is gradually stretched. This is because the unburned premixed gas does not reach the combustible temperature in the porous media region and is pushed to the downstream region for combustion, resulting in the flame shape stretching from an elliptical shape to a conical structure.

Figure 5 shows the characteristics of the axial temperature change of the fire tube during the stable combustion of methane and air at different equivalence ratios. Where STD represents the standard deviation of the axial temperature at different equivalence ratios. With the increase of the equivalence ratio, the maximum combustion temperature increases and then decreases, and the maximum combustion temperature of methane is the highest when the equivalence ratio is 0.7. This is because as the equivalence ratio increases, the fuel composition in the premixed gas increases, the heat released per unit time increases, and the maximum temperature rises to the limit. However, with a further increase in the equivalence ratio, the oxygen content in the premixed gas decreases, making the combustion incomplete. So, the maximum temperature of combustion decreases to some extent.

3.1.2. Effect of Porous Media Porosity. The porosity of the porous media is a key factor affecting combustion character-

https://doi.org/10.1021/acsomega.3c10444
ACS Omega 2024, 9, 31384−31392

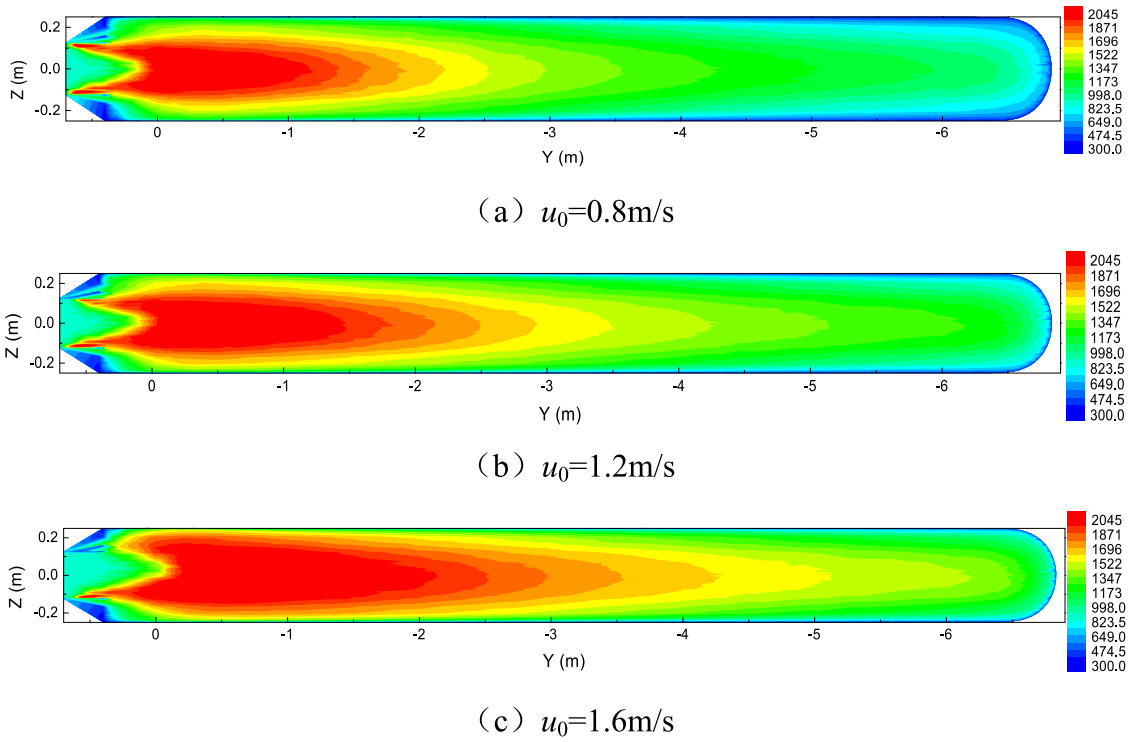

Figure 4. Comparison of temperature between different inlet velocities at Φ = 0.5: (a) u_0 = 0.8 m/s; (b) u_0 = 1.2 m/s; and (c) u_0 = 1.6 m/s.

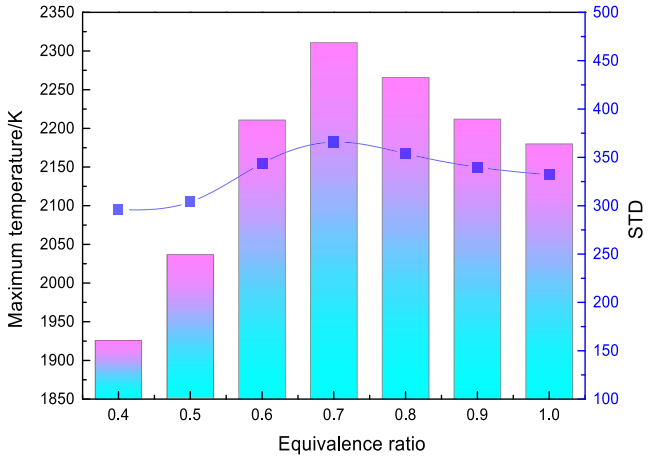

Figure 5. Effect of equivalence ratio on central axial temperature and standard deviation of axial temperature.

istics. The distribution of combustion heat can be effectively achieved by rationally arranging the porosity of porous media.[36] Figure 6a reflects the effect of porosity on the axial temperature in the center of the combustion chamber at an equivalence ratio of 0.8, an inlet velocity of 1.2 m/s, and a porous media thickness of 400 mm. The presence of porous media is more effective in improving the combustion efficiency of the fuel than in the absence of porous media.[37] The axial temperature distribution at the center of the porous media increases gradually with the increase in porosity in the interval −2.5 to 1 m. However, it can be found that the outlet radial temperature distribution becomes uniform with the increase of porosity from Figure 6b. And the peak temperature difference gradually decreases with the increase of porosity. The main reason is that with the increase of porosity, the pore diameter becomes smaller, and the flame is easier to be divided into small fragments. The combustion in the radial direction is more uniform. So, the flame area is more concentrated, which results in the axial temperature difference in the interval of −2.5 to 1 m but a uniform radial temperature distribution at the exit. On the other hand, the increase in porosity reduces the gas flow rate, prolongs the residence time of the flue gas in the fire tube, and enhances the heat exchange. The results showed that the peak temperature difference at the exit of the combustion chamber decreased with the increase of porosity.[32]

3.1.3. Effect of Porous Media Thickness. As can be seen in Figure 7a, the center axial temperature distribution is similar in the absence of porous media and 200 mm of porous media. This is mainly due to the larger inlet velocity, resulting in part of the gas passing through the porous medium region and insufficient combustion. Therefore, the difference in temperature distribution between no porous media and porous media is small by 200 mm, and the axial temperature is relatively low. When the thickness of the porous media is 300−600 mm, the temperature peak gradually increases with the increase of the thickness of the porous media. However, it can be seen from Figure 7b that the outlet temperature decreases with the increase of porous media thickness at 500 and 600 mm. The main reason for this is that in the case of a certain inlet velocity and equivalence ratio, an equal amount of heat released from the fuel can be returned to the upstream region by means of heat reflux. So that part of the heat in the flue gas is returned to the upstream region to preheat the unburned gas, thus increasing the combustion temperature. However, as the thickness of the porous media increases, the inertial and viscous resistances brought about by the porous media increase, the gas flow rate decreases, and the residence time in the fire tube is too long, leading to an increase in the heat dissipated to the outside world and accelerating the temperature drop in the combustor.[38]

https://doi.org/10.1021/acsomega.3c10444
ACS Omega 2024, 9, 31384−31392

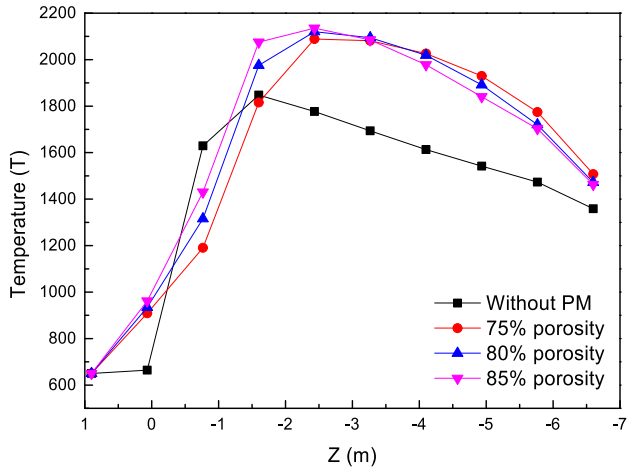

(a) Effect of porosity on central axial temperature

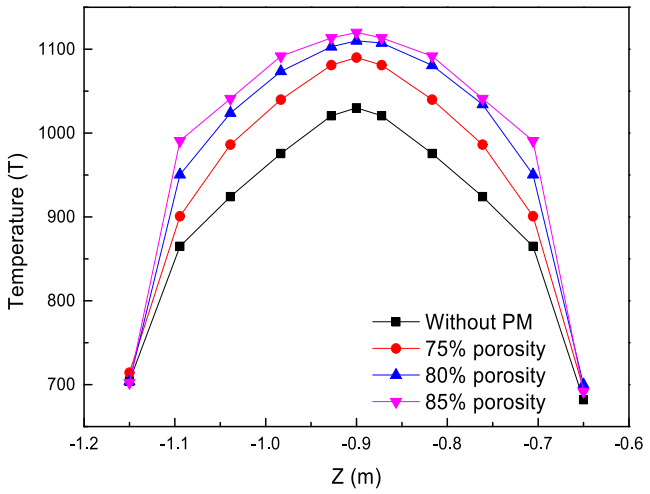

(b) Effect of porosity on outlet radial temperature

Figure 6. Effect of porosity on the outlet radial and central axial temperature.

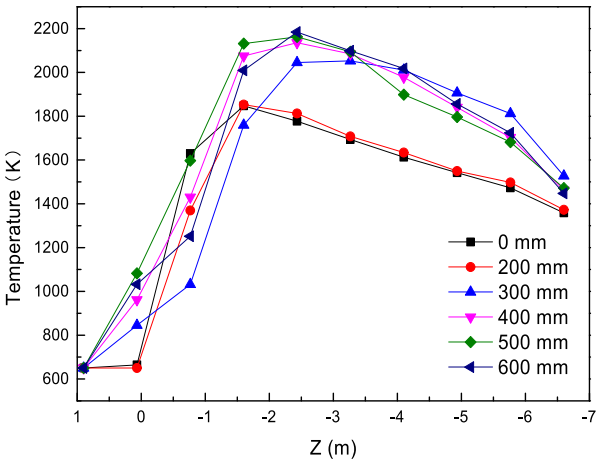

(a) Effect of media thickness on central axial temperature

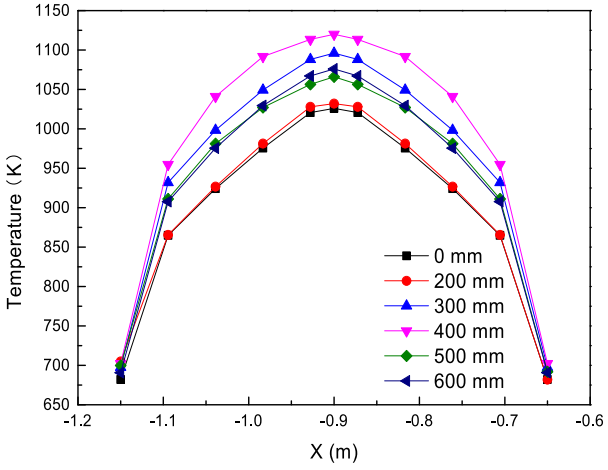

(b) Effect of media thickness on outlet radial temperature

Figure 7. Effect of media thickness on outlet radial and central axial temperature.

3.2. Comparison of NO Emission Characteristics. *3.2.1. Effect of Inlet Velocity and Equivalence Ratio.* Figure 8a shows the mass fraction distribution of NO under the conditions of equivalence ratio Φ = 0.5 and u_0 = 0.8−1.2 m/s. It can be seen from the figure that the NO is mainly concentrated in the high-temperature region. And its mass fraction shows a decreasing trend within the porous media and is gradually smoothed along the axial position. From the NOx emission mechanism, it can be seen that NO is affected by the temperature and the time of flue gas flow through the high-temperature region and the oxygen concentration.[24] At a certain equivalence ratio, NO emissions first decreased and then increased with an increase in inlet velocity. It was mainly due to the fact that with the increase of inlet velocity, the residence time of methane in the firebox was reduced despite the increase of combustion temperature.[39] It suppresses NO emissions. However, the increase in combustion intensity leads to an increase in combustion temperature inside the firebox, which becomes the dominant factor affecting NO production.[40] Therefore, this is more favorable to NO production.

Figure 8b shows the simulation results of NO emission characteristics during the stable combustion of methane and air premixed gases in porous media at different equivalence ratios. As can be seen from Figure 8b, under the condition of equivalence ratio Φ = 0.5:0.9, NO is generated in the high-temperature region, significantly reduced in the porous media region, and then smoothly decreased in the porous media. With the increase of the equivalence ratio, the NO mass fraction decreases gradually. And when the equivalence ratio increases from 0.5 to 0.9, the NO mass fraction at the exit of the fire hose decreases from 2.88×10^{-4} to 3.96×10^{-5}, which is a decrease of 86.5%. Based on the detailed chemical reaction mechanism, it is known that this is a reduction reaction of a small portion of NO under dilute combustion conditions, resulting in a decrease in NO concentration.[41]

3.2.2. Effect of Porous Media Porosity. Figure 9 shows the relationship between NO generation and the porosity of pollutants at an equivalence ratio of 0.8 and an inlet velocity of 1.2 m/s. It can be found that the NO emission is positively correlated with the center axial temperature distribution. The NO generation is mainly related to the combustion temperature, equivalence ratio, and the residence time of the flue gas in the high-temperature region.[42] The effect of the equivalence

https://doi.org/10.1021/acsomega.3c10444
ACS Omega 2024, 9, 31384−31392

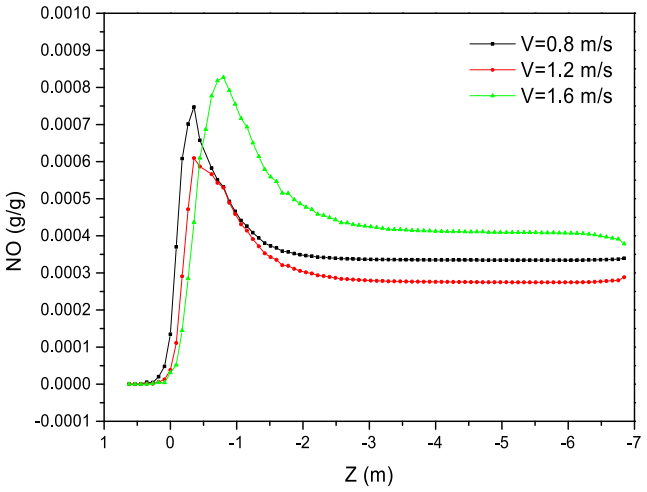

(a) Effect of inlet velocity on NO emissions

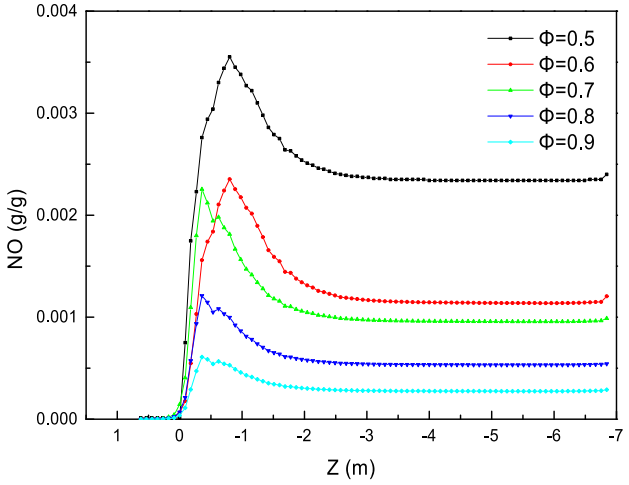

(b) Effect of equivalence ratio on NO emissions

Figure 8. Effect of input parameters on NO emissions.

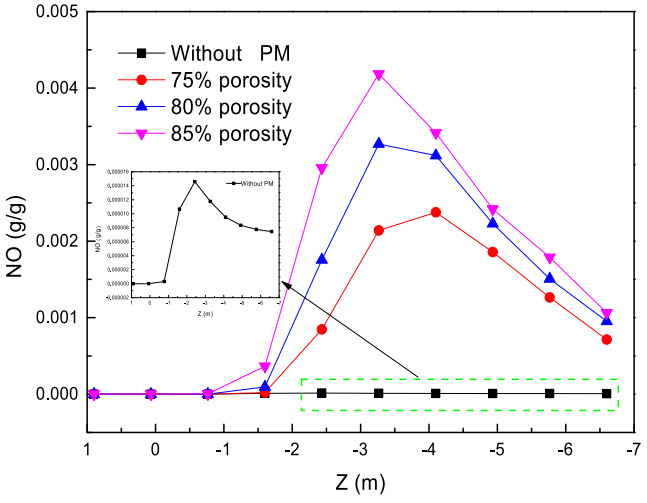

Figure 9. Effect of the porous media porosity on NO emissions.

ratio on NO generation can be ruled out for a certain excess air coefficient. It can be seen that NO generation increases with increasing porosity because porosity affects the combustion temperature and the residence time of the flue gas in the high-temperature region.[43]

3.2.3. Effect of Porous Media Thickness. Figure 10 shows the axial distribution of the NO concentration along the center

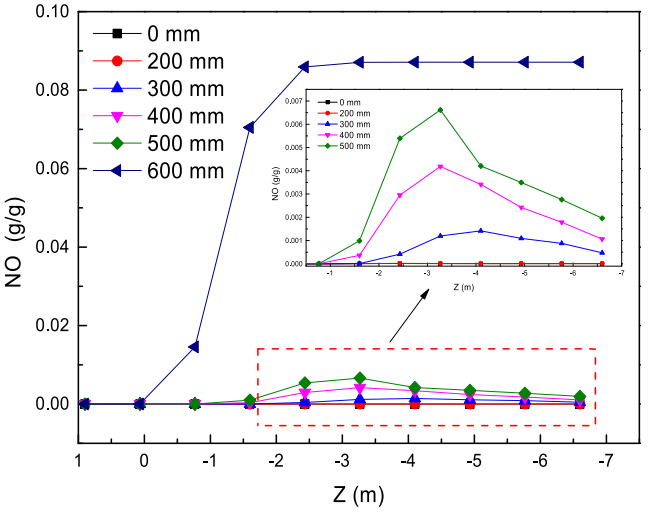

Figure 10. Effect of the porous media thickness on NO emissions.

of the combustor for different porous media thicknesses. It can be seen that in the porous media thickness of 0 to 500 mm, NO generation increases and then decreases as the distance from the combustor position increases. In the porous media thickness of 600 mm, NO generation increased with the growth of the position from the combustor and then stabilized. NO generation peak gradually increased, whereas in the porous media thickness of 600 mm, there is a sharp increase. The main reason is that with the increase of the length from the combustor, the temperature shows a tendency of increasing and then decreasing, which leads to an increase and then a decrease in the generation of thermal NO.[44] Then, the peak combustion temperature of the fuel increases due to the increase in the thickness of the porous media, leading to an increase in the production of thermal-type NO. Thus, as the thickness of the porous medium increases, the NO production also increases.[24,45]

4. CONCLUSIONS

A simulation study of methane-air combustion characteristics and NO emission patterns of a high-power porous media combustor of 800 to 1200 kW was carried out. The effects of inlet velocity, equivalence ratio, porosity, and porous media thickness on the combustion characteristics and NO emission patterns were analyzed. The results show that

(1) Porous media combustor in the equivalence ratio of Φ = 0.5−0.9 and the inlet velocity of 0.8−1.6 m/s range of stable combustion, and in the role of porous media, the fire tube in the center of the axial temperature distribution is more uniform.
(2) Increasing the inlet velocity (0.8−1.6 m/s) can expand the high-temperature region in the fire tube; the effect of equivalence ratio (Φ = 0.5−0.9) on the combustion temperature characteristics of methane-air porous media

https://doi.org/10.1021/acsomega.3c10444
ACS Omega 2024, 9, 31384−31392

is not linear, that is, when the equivalence ratio is 0.7, the highest value of combustion temperature occurs. The temperature in the interval from −2.5 to 1 m increases gradually with the increase of porosity. The radial temperature distribution at the outlet becomes uniform with the increase of porosity, and the peak temperature difference decreases gradually with the increase of porosity. The peak value of the exit temperature of the porous media appears to increase and decrease first, and the exit temperature is the highest in the porous media of 400 mm thickness.

(3) In the range of equivalence ratios (Φ = 0.5−0.9), NO emission decreases with the increase of equivalence ratios; in the range of inlet velocities from 0.8 to 1.6 m/s, NO emission is lowest when the inlet velocity is 1.2 m/s. In the range of porosity 0.75−0.85, NO production increases with increasing porosity. As the thickness of the porous media increases, NO generation increases, and a dramatic increase in NO generation occurs at 600 mm for the porous media.

(4) Controlling the thickness of the porous media can effectively reduce NO production in a high-power porous media combustor at a certain inlet flow rate and equivalence ratio. Controlling the porosity can improve the uniformity of temperature distribution in the fire tube of the high-power porous media combustor.

AUTHOR INFORMATION

Corresponding Author

Riyi Lin − *College of New Energy, China University of Petroleum (East China), Qingdao 266580, P. R. China;* orcid.org/0000-0002-7086-8919; Email: linry@upc.edu.cn

Authors

Wei Li − *College of New Energy, China University of Petroleum (East China), Qingdao 266580, P. R. China; Shengli Oilfield Technical Inspection Center, SlNOPEC, Dongying 257000, P. R. China*

Huanan Li − *College of New Energy, China University of Petroleum (East China), Qingdao 266580, P. R. China*

Xinxin Liu − *College of New Energy, China University of Petroleum (East China), Qingdao 266580, P. R. China*

Jitao He − *PetroChina (Xinjiang) Petroleum Engineering Co., Ltd., Karamay 834000, P. R. China*

Xinwei Wang − *College of New Energy, China University of Petroleum (East China), Qingdao 266580, P. R. China*

Complete contact information is available at: https://pubs.acs.org/10.1021/acsomega.3c10444

Author Contributions

R.L.: Supervision & writing—original draft. W.L.: Writing—original draft. H.L.: Writing—original draft. X.L.: Software. J.H.: Investigation. X.W.: Writing—review and editing.

Notes

The authors declare no competing financial interest.

ACKNOWLEDGMENTS

This work was supported by the National Natural Science Foundation of China (No. 5187433), Shandong Provincial Natural Science Foundation (ZR2021QE051), and Fundamental Research Funds for the Central Universities (22CX06030A, 20CX06028A).

REFERENCES

(1) Kumar, G.; Kim, S. H.; Lay, C. H.; Ponnusamy, V. K. Recent developments on alternative fuels, energy and environment for sustainability. *Bioresour. Technol.* **2020**, *317* ((4)), No. 124010.

(2) Stančin, H.; Stanin, H.; Mikulčić, H.; Kuli, H.; Wang, X. A review on alternative fuels in future energy system. *Renewable Sustainable Energy Rev.* **2020**, *128*, No. 109927.

(3) Weinberg. Combustion temperatures: the future? *Nature* **1971**, *233* (5317), 239−241.

(4) Banerjee, A.; Paul, D. Developments and applications of porous media combustion: A recent review. *Energy* **2021**, *221*, No. 119868.

(5) Boigné, E.; Zirwes, T.; Parkinson, D. Y.; et al. Integrated experimental and computational analysis of porous media combustion by combining gas-phase synchrotron μCT, IR-imaging, and pore-resolved simulations. *Combust. Flame* **2024**, *259*, No. 113132.

(6) Zhdanok, S.; Kennedy, L. A.; Koester, G. Superadiabatic combustion of methane air mixtures under filtration in a packed bed. *Combust. Flame* **1995**, *100*, 221−231.

(7) Bakry, A. I.; Mehrez, O.; Yahya, S. M. Effect of quenching region characteristics on the performance of two-region porous inert medium combustors at low-power operation. *Fuel* **2023**, *334*, No. 126638.

(8) Hashemi, S. M.; Hashemi, S. A. Flame stability analysis of the premixed methane air combustion in a two layer porous media combustor by numerical simulation. *Fuel* **2017**, *202*, 56−65.

(9) Zheng, C. H.; Cheng, L. M.; Li, T.et al. Numerical Simulation of Flame Surface Characteristics in Porous Media *Proceedings of the CSEE* 2009; Vol. *29* 05.

(10) Shinoda, M.; Yamada, E.; Kajimoto, T.; et al. Mechanism of magnetic field effect on OH density distribution in a methane air premixed jet flame. *Proc. Combust. Inst.* **2005**, *30* (1), 277−284.

(11) Yang, S. I.; Hsu, D. L. Heat-transfer mechanisms of lean premixed CH4/air flame in a ceramic granular bed burner. *Combust. Flame* **2013**, *160* (3), 692−703.

(12) Yan, H.; Du, T. J.; Peng, G. L. Microscopic simulation of heat transfer characteristics in porous media. *Mod. Appl. Phys.* **2017**, *8* (2), 7.

(13) Sasmal, A.; Mishra, S. C. Analysis of Conduction and Radiation Heat Transfer in a Differentially Heated 2-D Square Enclosure. *Heat Transfer* **2017**, *46*, 384−408, DOI: 10.1002/htj.21221.

(14) Zhao, C.; Lu, T.; Hodson, H.; et al. The temperature dependence of effective thermal conductivity of open-celled steel alloy foams. *J. Mater. Sci. Eng. A* **2004**, *367*, 123−131.

(15) Chu, J. H.; Cheng, L. M.; Shi, Z. L.; et al. Experimental study on gradual porous media gas Plant. *Combust. Sci. Technol.* **2009**, No. 1, 7.

(16) Xie, B.; Peng, Q.; Shi, Z.; et al. Investigation of CH4 and porous media addition on thermal and working performance in premixed H2/air combustion for micro thermophotovoltaic. *Fuel* **2023**, *339*, No. 127444.

(17) Wang, Q.; Ma, H.; Shen, Z.; Guo, Z. Numerical Simulation of Premixed Methane-air Flame Propagating Parameters in Square Tube with Different Solid Obstacles. *Procedia. Eng.* **2013**, *62*, 397−403.

(18) Gao, H.; Qu, Z.; Tao, W.; et al. Experimental Study of Biogas Combustion ina Two-Layer Packed Bed Combustor. *Energy Fuels* **2011**, *25* (7), 2887−2895.

(19) Shakiba; Sayed, S. A.; et al. Effects of foam structure and material on the performance of premixed porous ceramic burner. *Proc. Inst. Mech. Eng., Part A* **2015**, *229* (2), 176−191.

(20) Kang, S. H.; Wang, E. Y.; Zhao, C. T.; et al. Experimental study on building block inner core structure of ultra-low calorific value porous media combustor. *J. Hebei Univ. Technol.* **2018**, *47* (3), 7.

(21) Khanna, V.; Goel, R.; Ellzey, J. L. Measurements of Emissions and Radiation for Methane Combustion within a Porous media Combustor. *Combust. Sci. Technol.* **2016**, *99* (1−3), 133−142.

(22) Dehaj, M. S.; Ebrahimi, R.; Shams, M.; et al. Experimental Analysis of Natural Gas Combustion in a Porous Combustor. *Exp. Therm. Fluid Sci.* **2017**, *84*, 134−143.
(23) Büyükakın, M. K.; Öztuna, S. Study on nonpremixed methane/air combustion from flame structure and NOX emission aspect for different combustor head structures. *Int. J. Energy Res.* **2019**, *43* (10), 5421−5437.
(24) Keramiotis, C.; Stelzner, B.; Trimis, D.; et al. Porous combustors for low emission combustion: An experimental investigation. *Energy* **2012**, *45* (1), 213−219.
(25) Fierro, M.; Gutierrez, C.; Bubnovich, V.; et al. Thermal effect of hollow spheres in a filtration combustion process. *Appl. Therm. Eng.: Design, processes, equipment, economics* **2021**, *195* (195), No. 117037.
(26) Janvekar, A. A.; Abdullah, M. Z.; Ahmad, Z. A. et al. Investigation of micro combustor performance during porous media combustion for surface and submerged flames. **2018**, *3701* 012049. DOI: 10.1088/1757-899X/370/1/012049.
(27) Wang, W. J.; Zhou, Y. F.; Yao, J. H.; et al. Simulation of hetero/homogeneous combustion characteristics of CH4/air in a half packed-bed catalytic combustor. *Chem. Eng. Sci.* **2020**, *211*, No. 115247.
(28) Zhang, Y. X.; Gao, B. P. High altitude oxidation tank temperature field based on CFD numerical simulation. *J. Hydrometallurgy* **2022**, *9* (02), 170−175.
(29) Mohamed, I. A. Numerical investigation of natural convection in an inclined porous enclosure using non-Darcian flow model. *Int. J. Numer. Methods Heat Fluid Flow* **2019**, *30* (4), 1881−1897.
(30) Mohamed, I. A.; Kowsalya, M. Optimal size and siting of multiple distributed generators in distribution system using bacterial foraging optimization. *Swarm Evol. Comput.* **2014**, *15*, 58−65.
(31) Li, J.; Li, Q. Q.; Shi, J. R.; et al. Numerical study on heat recirculation in a porous micro-combustor. *Combust. Flame* **2016**, *171*, 152−161.
(32) Gao, H. B.; Qu, Z. G.; Feng, X. B.; et al. Methane/air premixed combustion in a two-layer porous combustor with different foam materials. *Fuel* **2014**, *115* ((1)), 154−161.
(33) Nicol, D. G.; Malte, P. C.; Hamer, A. J.; et al. Development of a five-step global methane oxidation-NO formation mechanism for lean-premixed gas turbine combustion. *J. Eng. Gas Turbines Power* **1999**, *121* (2), 272−280.
(34) Othman; Mohamed, M. I. A. Generalized Electromagneto-Thermoelastic Plane Waves by Thermal Shock Problem in a Finite Conductivity Half-Space with One Relaxation Time. *Multidiscip. Model. Mater. Struct.* **2005**, *1* (3), 231−250.
(35) Drayton, M. K.; Saveliev, A. V.; Kennedy, L. A.et al. Syngas production using superadiabatic combustion of ultra-rich methane-air mixtures[C]. In *Symposium (International) on Combustion*; Elsevier, 1998; Vol. *27*, pp 1361−1367.
(36) Dagaut, P.; Dayma, G.; Nicolle, A. Experimental and detailed chemical kinetic modeling study of the oxidation of hydrogen-enriched natural gas blends. In *European Combustion Meeting*; ECM, 2005.
(37) Mujeebu, M. A.; Abdullah, M. Z.; Bakar, M. Z.; et al. Combustion in porous media and its applications−A comprehensive survey. *J. Environ. Manage.* **2009**, *90* (8), 2287−2312.
(38) Qu, Z.; Gao, H.; Feng, X.; et al. Premixed combustion in a porous combustor with different fuels. *Combust. Sci. Technol.* **2015**, *187* (3), 489−504.
(39) Farzaneh, M.; Ebrahimi, R.; Shams, M.; et al. Numerical simulation of thermal performance of a porous burner. *Chem. Eng. Process.: Process Intensif.* **2009**, *48* (2), 623−632.
(40) Hashemi, S. A.; Nikfar, M.; Ghorashi, S. A. Numerical study of the effect of thermal boundary conditions and porous media properties on the combustion in a combined porous-free flame burner. *Proc. Inst. Mech. Eng., Part A* **2018**, *232* (7), 799−811.
(41) Ghorashi, S. A.; Hashemi, S. A.; Hashemi, S. M.; et al. Experimental study on pollutant emissions in the novel combined porous-free flame burner. *Energy* **2018**, *162*, 517−525.
(42) Zhou, X. Y.; Pereira, J. C. Numerical study of combustion and pollutants formation in inert nonhomogeneous porous media. *Combust. Sci. Technol.* **1997**, *130* (1−6), 335−364.
(43) Liu, H.; Dong, S.; Li, B. W.; Chen, H. G. Parametric investigations of premixed methane−air combustion in two-section porous media by numerical simulation. *Fuel* **2010**, *89* (7), 1736−1742.
(44) Zhang, J.; Cheng, L.; Zheng, C.; et al. Numerical Studies on the Inclined Flame Front Break of Filtration Combustion in Porous Media. *Energy Fuels* **2013**, *27* (jul.-aug.), 4969−4976.
(45) Djordjevic, N.; Habisreuther, P.; Zarzalis, N. Experimental Study on the Basic Phenomena of Flame Stabilization Mechanism in a Porous Combustor for Premixed Combustion Application. *Energy Fuels* **2012**, *26* (11), 6705−6719.

https://doi.org/10.1021/acsomega.3c10444
ACS Omega 2024, 9, 31384−31392